

CHEMISTRY

A European Journal

A Journal of



Accepted Article

Title: Fluorine-substituted molecular motors with a quaternary stereogenic center

Authors: Peter Štacko, Jos C. M. Kistemaker, and Ben Lucas Feringa

This manuscript has been accepted after peer review and appears as an Accepted Article online prior to editing, proofing, and formal publication of the final Version of Record (VoR). This work is currently citable by using the Digital Object Identifier (DOI) given below. The VoR will be published online in Early View as soon as possible and may be different to this Accepted Article as a result of editing. Readers should obtain the VoR from the journal website shown below when it is published to ensure accuracy of information. The authors are responsible for the content of this Accepted Article.

To be cited as: *Chem. Eur. J.* 10.1002/chem.201700581

Link to VoR: <http://dx.doi.org/10.1002/chem.201700581>

Supported by
ACES

WILEY-VCH

Fluorine-substituted molecular motors with a quaternary stereogenic center

Peter Štacko^[a], Jos C. M. Kistemaker^[a] and Ben L. Feringa^{*[a]}

Abstract: A series of unprecedented second generation molecular motors featuring a quaternary stereogenic center substituted with a fluorine atom has been synthesized. It is demonstrated that a seemingly benign replacement of the stereogenic hydrogen for a fluorine atom, regarded as a common substituent in pharmacology, resulted in a dramatic change in the energetic profile of thermal helix inversion. The barrier for the thermal helix inversion was found to increase considerably (by 20–30 kJ·mol⁻¹), presumably due to destabilization of the transition state by increased steric hindrance when the fluorine atom is forced to pass over the lower half of the motor. This results in the activation barrier for the thermal helix inversion to be higher than the barrier for backward thermal *E-Z* isomerization, impairing the motor function. A fluorine-substituted motor capable of performing unidirectional rotation is successfully prepared when these limitations are considered in the design phase.

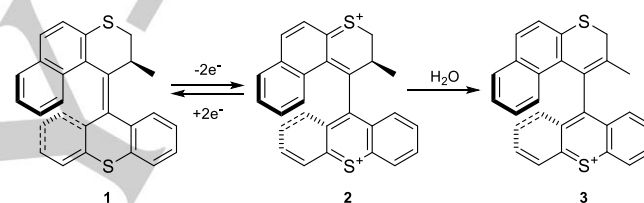
Introduction

On a daily basis, we are fortunate to witness the impressive collection of molecular machines and nanosystems developed by Nature to operate complex biological processes responsible for various key functions in living organisms.^[1,2] Complimenting the level of sophistication and elegance that evolved within the design of these systems, the ability of Nature to harness the proton gradient across a membrane to drive the rotation of the axle in the ATPase motor^[3–6] or to drive flagella of bacteria^[7–10] has served as inspiration for scientists to achieve redox-driven molecular motion in a controlled fashion.^[11–14] The importance of achieving molecular machine functions utilizing redox switching^[15–21] was recognized as it promises to allow single or small groups of molecules to be addressed more easily than with a either chemical fuel or with light.^[22–24]

For example, Sauvage and co-workers reported that changes in the [copper(I)/(II)] redox state resulted in a change of the coordination number, leading to rotation of two interlocked rings in a catenane.^[15] An alternative approach adopted by Stoddard and co-workers exploited the change of the affinity of a moiety in a rotaxane, inducing translational motion upon a change in its redox state.^[25] Alternatively, the structural changes observed during photochemical isomerization being mimicked by redox switching has been demonstrated for a molecular nanocar^[26], dithienylethene^[27,28], and spiropyran-based^[29–31] switches as well as dithienylethene switches immobilized^[32,33] on surfaces.

In the recent attempt of Logtenberg *et al.* to devise a unidirectional electrochemically driven molecular motor based on a second generation motor, it was observed that deprotonation at the stereogenic center results in double bond migration inside the upper rotor half and this constitutes the major degradation pathway since it leads to a release of the strain around the overcrowded double bond axle (Scheme 1).^[34] In that study, the molecular motor **1** was electrochemically oxidized to dication **2**. However, in the presence of water, **2** underwent irreversible deprotonation to restore aromaticity of the naphthalene moiety as confirmed by X-ray structure determination. The formation of side product **3** hindered further

application of the compound **1** as an electrochemically driven unidirectional molecular motor. Potentially blocking this position with an additional substituent and thus preventing the undesired deprotonation step could alleviate this issue and allow for the construction of a reversible redox-active and unidirectional molecular motor.



Scheme 1. Olefinic double bond shift inside the ring of the upper half upon electrochemical oxidation of the motor **1** to **2** in presence of traces of water.^[34]

Table 1. Selected thermodynamic and kinetic parameters for thermal helix inversion of second generation motors with various substituents at the stereogenic center.

R	$\Delta^{\ddagger}G^{\circ}$ [kJ·mol ⁻¹]	k (293 K) [s ⁻¹]	$t_{1/2}$ (293 K) [s]
Ph	88	1.18×10^{-3}	587
Me	85	3.64×10^{-3}	190
<i>i</i> -Pr	84	7.32×10^{-3}	95
<i>t</i> Bu	60	1.21×10^2	5.74×10^{-3}

Additional studies on the impact of structural modifications of the stereogenic center are imperative from other perspectives as well. Numerous derivatives of the upper and lower halves of the second generation motors have been made over the course of years in our group. Both first and second generation motors with five- and six- membered upper and lower halves have been synthesized and the consequences of such structural alterations on the motor properties have been evaluated.^[35–39] Few

[a] P. Štacko, J. C. M. Kistemaker, Prof. Dr. B. L. Feringa
Centre for Systems Chemistry, Stratingh Institute for Chemistry
University of Groningen
Nijenborgh 4, 9747 AG Groningen, The Netherlands
Fax: (+ 31) 50-363-4296
E-mail: b.l.feringa@rug.nl

Supporting information for this article is given via a link at the end of the document.

investigations into an important structural motif, the stereogenic center, have been made. Substituents distinct from the typical methyl group such as phenyl, *t*-butyl or methoxy groups have been reported for second generation motors (Table 1).^[35,38] From these investigations, it could be concluded that the activation barrier for the thermal helix inversion decreases as the relative bulk of the substituent at the stereogenic center increases. To the best of our knowledge, no reports with a quaternary stereogenic center on first or second generation molecular motors have been published.

Therefore, a functional molecular motor featuring a quaternary stereogenic center is valuable for certain applications that require a higher stability of the overcrowded alkenes; such as redox-driven systems or to serve as an additional tool for tuning the rotary speed of the motors. Quaternarization of the stereogenic center is not an easy task as an appreciable difference in size of the two substituents must be preserved in order to retain unidirectionality of the molecular motor. At the same time, increasing the steric hindrance in this position complicates synthesis; in particular functionalization of the corresponding ketone intermediate as well as the Barton-Kellogg coupling used for construction of the overcrowded alkenes. Based on these considerations, replacement of the hydrogen atom for fluorine was proposed since fluorine (71 pm) is "only" twice the size of hydrogen atom (37 pm)^[40] and is often considered a suitable replacement for hydrogen in pharmacology in order to improve stability or lipophilicity of lead compounds. To this end, we set out to synthesize fluoro-analogues of the second generation motor **4–6** (Figure 1).

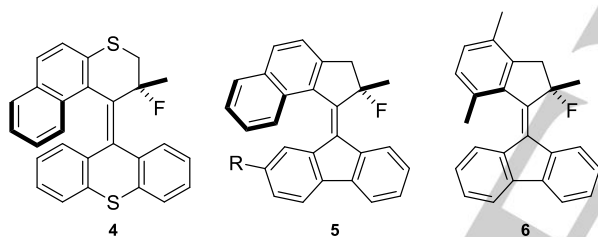


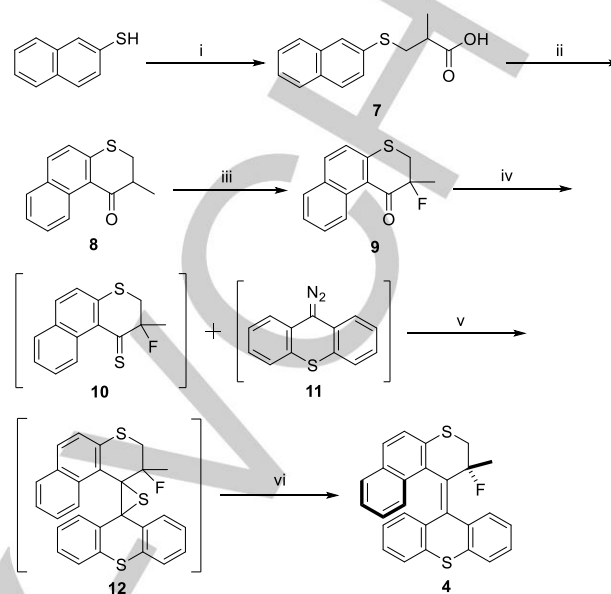
Figure 1. Target fluoro-analogues of previously reported second generation motors.

Results and Discussion

Synthesis

The synthesis of the fluorinated analogue of the second generation motor **4** started with preparation of the upper half **9** (Scheme 2). Previously, the synthesis of precursors started with a Michael addition of naphthalene-2-thiol to methacrylonitrile. However, due to safety issues, methacrylonitrile was no longer commercially available and a different synthetic sequence had to be conceived. Therefore, naphthalene-2-thiol was added in a Michael reaction to methacrylic acid in the presence of Et₃N (Scheme 2). The resulting carboxylic acid **7** was treated with oxalyl chloride and the resulting acyl chloride was subjected to an intramolecular Friedel-Crafts acylation in the presence of AlCl₃ to give the upper-half ketone **8** in excellent yield. Installation of the fluorine atom in the α -position was carried out by deprotonation with NaHMDS at -78 °C, followed by a reaction with NFSI in toluene. Different bases gave product **9** in lower or negligible yield, and the use of THF as a solvent led to

oxidation of the starting material into the corresponding α,β -unsaturated ketone, presumably via an SET mechanism.^[41–44]

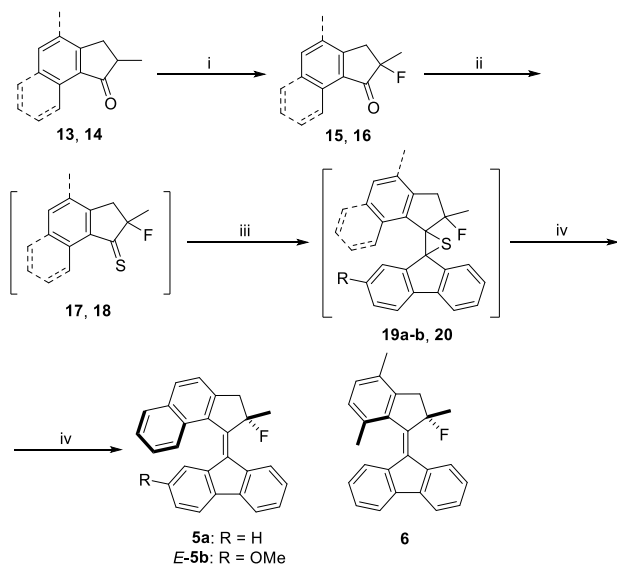


Scheme 2. Reaction conditions: (i) methacrylic acid, Et₃N, THF, 16 h, 79%; (ii) 1. (COCl)₂, DCM; 2. AlCl₃, DCM, 86%; (iii) 1. NaHMDS, toluene, -78 °C, 1 h; 2. NFSI, rt, 16 h, 67%; (iv) Lawesson's reagent, P₄S₁₀, toluene, 110 °C, 3 h; (v) THF, rt, 16 h; (vi) HMPT, toluene, 50 °C, 16 h, 17%.

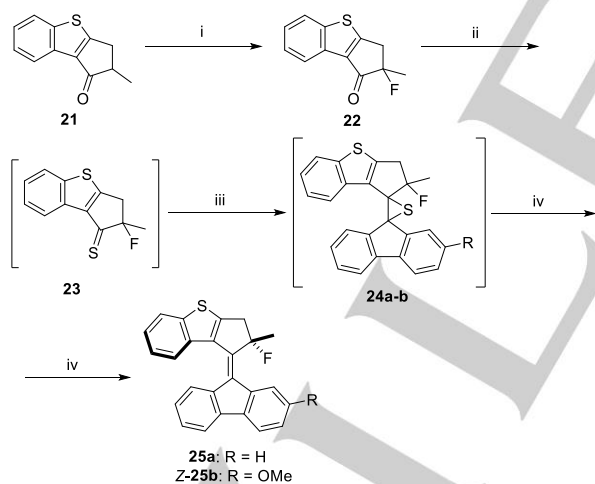
With the fluorinated ketone **9** in hand, transformation of the carbonyl into a hydrazone or a thioether was investigated. Reaction with NH₂NH₂·H₂O led to a complex reaction mixture, however, transformation of **9** into the thioether **10** could be carried out using a combination of P₄S₁₀ and Lawesson's reagent at reflux in toluene. Reaction times substantially longer than 3 h led to decomposition of the product. The thioether **10** was then reacted with freshly prepared diazo-compound **11** and the resulting episulfide **12** was to be desulfurized to give the target molecule **4**. Since PPh₃ was not reactive enough to promote the desulfurization in this hindered system, alternative methods had to be explored. After unsuccessful attempts with Zn/Cu/*p*-OMePh)₃P, HMPT was employed as a more reactive phosphine to facilitate the reaction. Interestingly, the resulting overcrowded alkene was found to be prone to oxidation into the corresponding dication during purification on silica gel.

The upper halves **13** and **14** for the purpose of further functionalization and synthesis of fluorinated motors **5a–b** and **6** were synthesized by a reaction of *p*-xylene or naphthalene with methacryloyl chloride in the presence of AlCl₃ at low temperature. The ketones **13** and **14** were fluorinated at the α -position using LiHMDS/NFSI in toluene in 83% and 85% yield, respectively (Scheme 3). Thionation of **15–16** with a mixture of P₄S₁₀ and Lawesson's reagent in toluene at reflux afforded the thioethers **17–18** that were immediately reacted with 9-diazo-9*H*-fluorene or its 2-methoxy derivative. The episulfides **19a–b** and **20** were conveniently desulfurized *in situ* with HMPT at room temperature. The motors **5a–b** and **6** were isolated in 49%, 25% and 50% yield, respectively, as yellow orange solids after column chromatography (silica gel) of the reaction mixture adsorbed on Celite. Prolonged exposure to silica gel, either during adsorption or column chromatography, resulted in partial

decomposition of the product. The motor **5b** was isolated as nearly pure *E*-isomer by repeated crystallization from ethanol. The *E*-geometry was assigned based on ^1H NMR absorption of the methoxy group (δ (ppm) = 2.92 ppm) in analogy with reported second generation motors.^[45,46]



Scheme 3. Reaction conditions: (i) 1. LiHMDS, toluene, $-78\text{ }^\circ\text{C}$, 1 h; 2. NFSI, rt, 16 h, 83–85%; (ii) Lawesson's reagent, P_4S_{10} , toluene, $110\text{ }^\circ\text{C}$, 1 h; (iii) 9-diazo-9*H*-fluorene or 9-diazo-2-methoxy-9*H*-fluorene, toluene, rt, 16 h; (iv) HMPT, toluene, rt, 16 h; **5a**: 49%, **E-5b**: 49%, **6**: 50% over 3 steps.



Scheme 4. Reaction conditions: (i) 1. LiHMDS, toluene, $-78\text{ }^\circ\text{C}$, 1 h; 2. NFSI, rt, 16 h, 38%; (ii) Lawesson's reagent, P_4S_{10} , toluene, $110\text{ }^\circ\text{C}$, 1 h; (iii) 9-diazo-9*H*-fluorene or 9-diazo-2-methoxy-9*H*-fluorene, toluene, rt, 16 h; (iv) HMPT, toluene, rt, 16 h; **25a**: 61%, **Z-25b**: 54% over 3 steps.

The upper half ketone **21** based on a benzo[*b*]thiophene moiety was previously synthesized from benzo[*b*]thiophene and methacrylic acid in PPA. This procedure leads to a mixture of two regioisomers that are difficult to separate by column chromatography and only the use of a slow gradient of eluent

leads to partial separation of the regioisomers. Installation of the fluorine atom proved to be not as straightforward as for previous molecules. In general, the reaction of **21** with NFSI suffered from poor and variable conversion, combined with poor separation of the product from the starting material which substantially lowered the yield. The yield was also highly dependent on the quality of the solvent and NFSI. Different reagents used for electrophilic fluorination such as *N*-fluoropyridinium salts or Selectfluor did not lead to the desired product. At this point, the ketone **22** was converted into the thioether **23** with a mixture of P_4S_{10} and Lawesson's reagent in toluene at reflux. After purification by quick column chromatography, the thioether **23** was immediately reacted with 9-diazo-9*H*-fluorene or its 2-methoxy derivative to give the episulfides **24a-b**, which were desulfurized *in situ* with HMPT to give the final motor **25a** and the desymmetrized analogue **25b** with an *Z*-configuration. The geometry of **25b** was assigned based on the ^1H NMR resonance of the methoxy group (δ (ppm) = ~ 3.90 ppm) in analogy with reported motors.^[45,46]

Photochemical and thermal isomerizations

The photochemical and thermal behavior of **4** was examined in solution using UV-vis absorption in order to understand the influence of quaternarization of the stereogenic center on these processes. The UV-vis absorption spectrum of the fluorinated motor **4** in heptane at 293 K shows an absorption band centered at 392 nm (Figure 2, black). Irradiation of the sample with UV light (365 nm) under ambient conditions led to the formation of a broad band between 500 and 550 nm with two local maxima. Identical spectral changes were observed throughout the electrochemical experiments of the parent desfluoro compound **1**^[34], suggesting a photooxidation to the dication **2** is taking place. The solution of **4** was therefore deoxygenated with three freeze-pump-thaw cycles and irradiation with UV light (365 nm) was repeated. In this case, an increase of intensity of the band at 392 nm was observed (Figure 2, blue). This observation is consistent with a formation of the unstable form of second generation motors. The irradiation was continued until the photostationary state (PSS) was reached. Leaving the sample to stand in the dark or heating the sample to 363 K for 16 hours resulted in a complete retention of the band at 391 nm (Figure 2, red dashed). The initial spectrum was not recovered, indicating a very high barrier for the anticipated thermal helix inversion (THI), compared to the barrier of $105.6\text{ kJ}\cdot\text{mol}^{-1}$ reported for the parent compound.^[46]

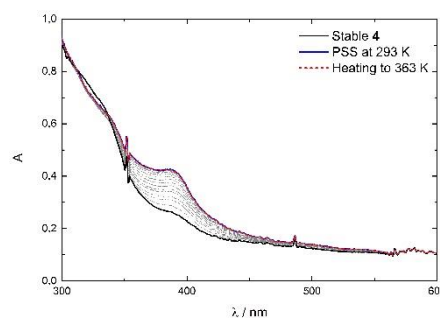


Figure 2. UV-vis absorption spectra (heptane, 293 K, $c = \sim 4 \times 10^{-5}$ M). Stable **4** (black solid); irradiation to PSS at 293 K (blue solid); after heating the sample to 363 K for 16 h (dashed red).

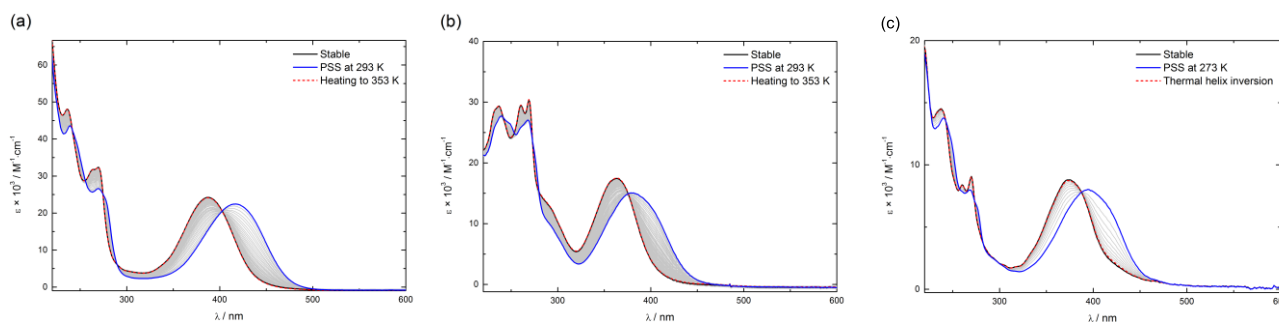


Figure 3. UV-vis absorption spectra (heptane, 293 K, $c = \sim 2\text{--}4 \times 10^{-5}$ M). (a) stable **5a** (black solid); irradiation to PSS at 293 K (blue solid); after heating the sample to 353 K (dashed red). (b) stable **6** (black solid); irradiation to PSS at 293 K (blue solid); after heating the sample to 353 K (dashed red). (c) stable **25a** (black solid); irradiation to PSS at 273 K (blue solid); after heating the sample to 293 K (dashed red).

In order to verify the hypothesis that installation of the fluorine atom at the stereogenic center leads to a large increase of the barrier for thermal helix inversion, two fluoro-substituted motors **5** and **6**, derived from second generation motors with much lower barriers for THI, were proposed. It was assumed that since the THI barrier for the desfluoro analogues is fairly low, the measurement of activation parameters for THI will still be possible despite the anticipated significant increase of the barrier induced by the introduction of a fluorine atom in the molecules.

The fluorinated analogues **5** and **6** were therefore synthesized (Scheme 3, *vide infra*) and their photochemical and thermal behavior was investigated in solution using UV-vis absorption, ^1H and ^{19}F NMR spectroscopy. The UV-vis absorption spectra of the motors **5** and **6** in heptane at 293 K show absorption bands centered at 387 and 363 nm, respectively (Figure 3a-b, solid black). Irradiation of the samples with UV light (365 nm) under ambient conditions resulted in the emergence of bathochromically shifted absorption bands at 417 and 379 nm, respectively, indicating the formation of the unstable forms of motors **5** and **6** (Figure 2a-b, blue solid). Throughout the irradiation, a single isosbestic point was observed in each case. After the PSS was reached, the samples were heated at 353 K for several hours and full reversal to the original UV-vis spectra was observed, indicating that either the anticipated thermal helix inversion or an undesired backward thermal *E-Z* isomerization is taking place (Figure 3a-b, red dashed). The UV-vis absorption spectra of the desymmetrized motor *E-5b* in heptane at 293 K and its photochemical/thermal behavior was found to be nearly identical to that of **5a** (see SI, Figure S31).

The rate constants for the thermal isomerization were measured at five different temperatures between 333 and 358 K by following the change in UV-vis absorption spectra over time. Multivariate analysis was performed on the array of the spectra, providing the rate constant for each temperature. The Eyring plot was then constructed and the activation parameters for the thermal process were derived from the linear fit (see SI, Figure S32 and S33). The Gibbs free energy of activation $\Delta^\ddagger G^\circ$ for thermal isomerization of the unstable **5a** back to the stable **5a** was found to be 106.2 ± 0.2 $\text{kJ}\cdot\text{mol}^{-1}$, corresponding to a half-life of 11.1 ± 1.1 days at room temperature (Table 2). In the case of **6**, the Gibbs free energy of activation $\Delta^\ddagger G^\circ$ for thermal isomerization of the unstable **6** back to the stable **6** was found to be 104.3 ± 0.3 $\text{kJ}\cdot\text{mol}^{-1}$, corresponding to a half-life of 5.2 ± 0.5 days at room temperature (Table 2). Only a negligible influence of the methoxy substituent on the activation parameters of the thermal step was observed for **5b** (Table 2, Figure S33).

Table 2. Selected thermodynamic parameters of the thermal step for the motors **5a-b**, **6** and **25a** and their corresponding desfluoro analogues.

Motor	$\Delta^\ddagger G^\circ$ [$\text{kJ}\cdot\text{mol}^{-1}$]	$\Delta^\ddagger H^\circ$ [$\text{kJ}\cdot\text{mol}^{-1}$]	$\Delta^\ddagger S^\circ$ [$\text{J}\cdot\text{K}^{-1}\cdot\text{mol}^{-1}$]	$t_{1/2}(293\text{ K})$
5a	106.2 ± 0.2	106.0 ± 1.6	-0.8 ± 4.5	11.1 ± 1.1 d
5b	105.9 ± 0.3	102.9 ± 1.7	-10.6 ± 4.9	10.1 ± 1.2 d
desfluoro- 5a ^[47]	86.1	71.8	-48.7	4.3 min
6	104.3 ± 0.3	97.7 ± 1.9	-22.6 ± 5.7	5.2 ± 0.5 d
desfluoro- 6 ^[37]	79.1	n.d.	n.d.	15 s
25a	88.4 ± 0.0	65.1 ± 0.2	-79.5 ± 0.5	642 ± 1 s
desfluoro- 25a ^[47]	71.1	34.0	-126	520 ms

The observed values for **5** and **6** are in a stark contrast with those reported for the desfluoro^[37,48] analogues which were found to be 86.1 $\text{kJ}\cdot\text{mol}^{-1}$ and 79.1 $\text{kJ}\cdot\text{mol}^{-1}$, corresponding to half-lives of 190 and 15 s, respectively, reaffirming the hypothesis of a large increase of the THI activation barrier upon substitution at the stereogenic center. In both cases, the $\Delta^\ddagger G^\circ$ of the thermal isomerization is increased by 21–25 $\text{kJ}\cdot\text{mol}^{-1}$ upon fluorine substitution, presumably due to destabilization of the transition state in which the pseudoaxially oriented fluorine atom is forced to pass over the top of the lower half. Due to the difference in size of the fluorine and hydrogen atom (and length of the bond), it can be expected that the steric repulsion will be higher for the former case, hence the increase in the energy of the transition state, translating into an increase of $\Delta^\ddagger G^\circ$. At this point, due to enhanced activation energy for the thermal step, desymmetrization of the lower half was required to unequivocally establish whether the thermal process being observed is a backward thermal *E-Z* or indeed the thermal helix inversion. For this purpose, a methoxy substituent was introduced in motor **5b**.

The nature of the thermal step was probed using ^1H and ^{19}F NMR spectroscopy. A sample of *E-5b* in d_8 -toluene (Figure 4a, left) was prepared since in the preliminary experiments decomposition in CDCl_3 was observed upon irradiation and a

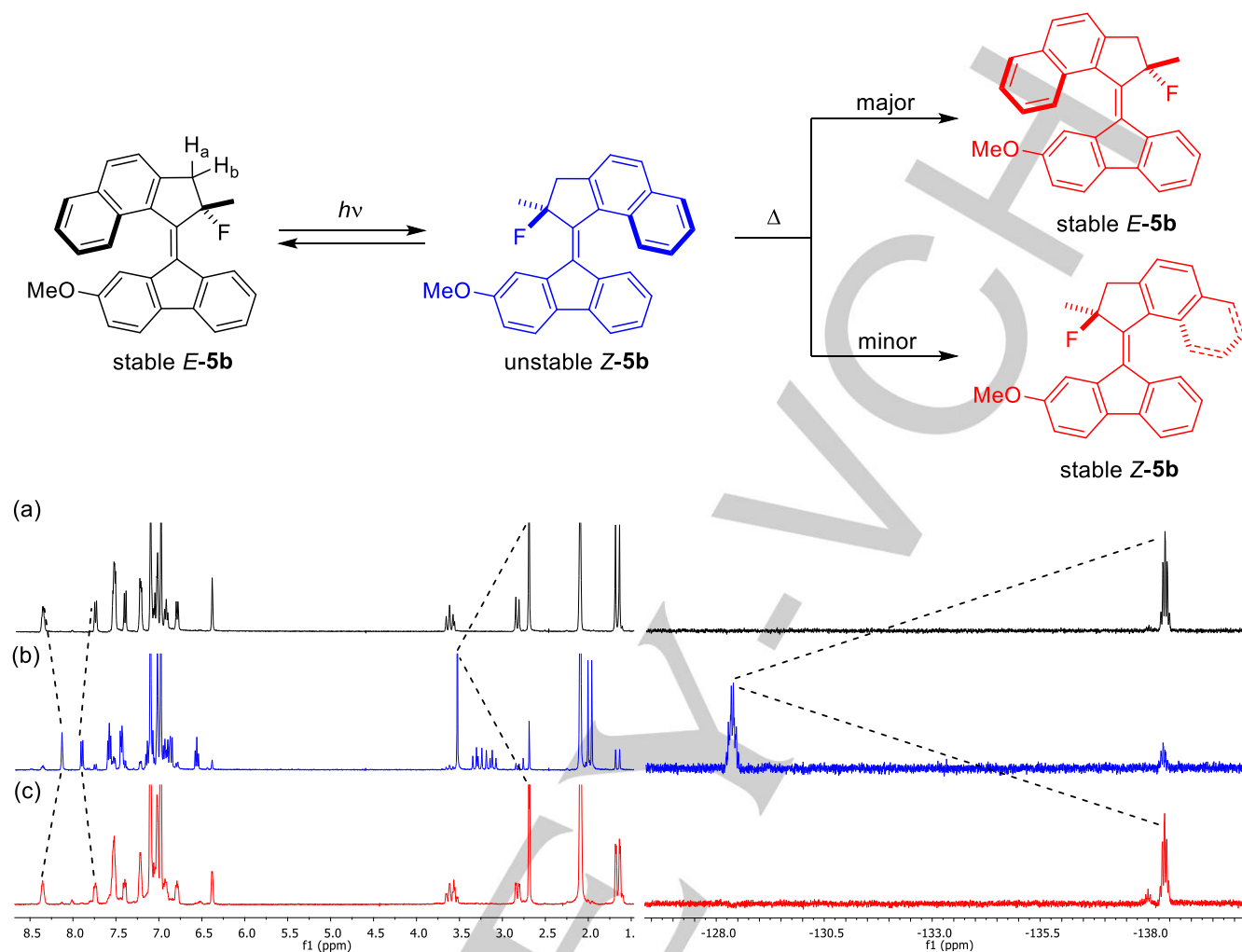


Figure 4. ^1H and ^{19}F NMR spectroscopy (400 MHz, d_6 -toluene, 293 K, $c = \sim 1 \times 10^{-2}$ M). (a) ^1H NMR (left) and ^{19}F NMR (right) of the stable *E*-5b. (b) irradiation (365 nm) to PSS and formation of the corresponding unstable *Z*-5b. (c) after heating to 323 K for 16 h mostly regeneration of the stable *E*-5b is observed.

higher temperature was required for the thermal isomerization. The sample was irradiated with UV-light (365 nm) at 293 K until PSS (85:15) was reached and ^1H and ^{19}F NMR spectra were recorded. The most significant change that occurred was a shift of the methoxy group resonance from 2.69 ppm to 3.53 ppm as a result of a photochemical *E-Z* isomerization of stable *E*-5b to unstable *Z*-5b. An upfield shift of H_a from 3.62 ppm to ~ 3.23 ppm and a downfield shift of H_b from 2.83 ppm to ~ 3.23 ppm was also observed (Figure 4b, left).

In the ^{19}F NMR spectrum, the formation of an additional resonance at -128.4 ppm was clearly observed (Figure 4b, right). These changes are consistent with formation of the unstable *Z*-5b. The sample was then heated to 323 K for 16 h and ^1H and ^{19}F NMR spectrum were recorded again (Figure 4c, left for ^1H NMR, right for ^{19}F NMR). Unfortunately, only about 10% of the expected stable *Z*-5b was observed and mostly regeneration of the stable *E*-5b was detected. Heating the unstable *Z*-5b at 348 K, the proportion of stable *Z*-5b changed to $\sim 27\%$. It could be concluded that the thermal step observed at this temperature can be attributed predominantly to the backwards thermal *E-Z* isomerization, with the thermal helix inversion being a minor pathway. As hypothesized earlier, it has been confirmed that the

installation of a fluorine atom at the stereogenic center increases the barrier for thermal helix inversion (>25 $\text{kJ}\cdot\text{mol}^{-1}$) to the extent that backwards thermal *E-Z* isomerization now becomes competitive.

The preceding experiments demonstrated that a scaffold with even less steric hindrance in the fjord region is required to preserve proper motor function upon introduction of fluorine. For this purpose, a benzothiophene-based upper-half was chosen, since it has been shown that the molecular motor featuring this upper-half possesses an extremely low barrier for thermal helix inversion ($\Delta^\ddagger G^\circ = 71.1$ $\text{kJ}\cdot\text{mol}^{-1}$, $t_{1/2}(298\text{ K}) = \sim 520$ ms).^[47] Such a low initial barrier should allow for considerable destabilization (up to ~ 30 $\text{kJ}\cdot\text{mol}^{-1}$) of the transition state of thermal helix inversion with respect to the unstable form, while still rendering the thermal *E-Z* isomerization noncompetitive. Based on this prediction, the fluorinated motor **25a** and its desymmetrized version **25b** with a benzothiophene upper-half were synthesized (Scheme 4, *vide supra*). Although less chemically stable than the predecessors **5a-b** or **6**, their photochemical and thermal behavior in solution was investigated using UV-vis absorption, ^1H and ^{19}F NMR spectroscopy.

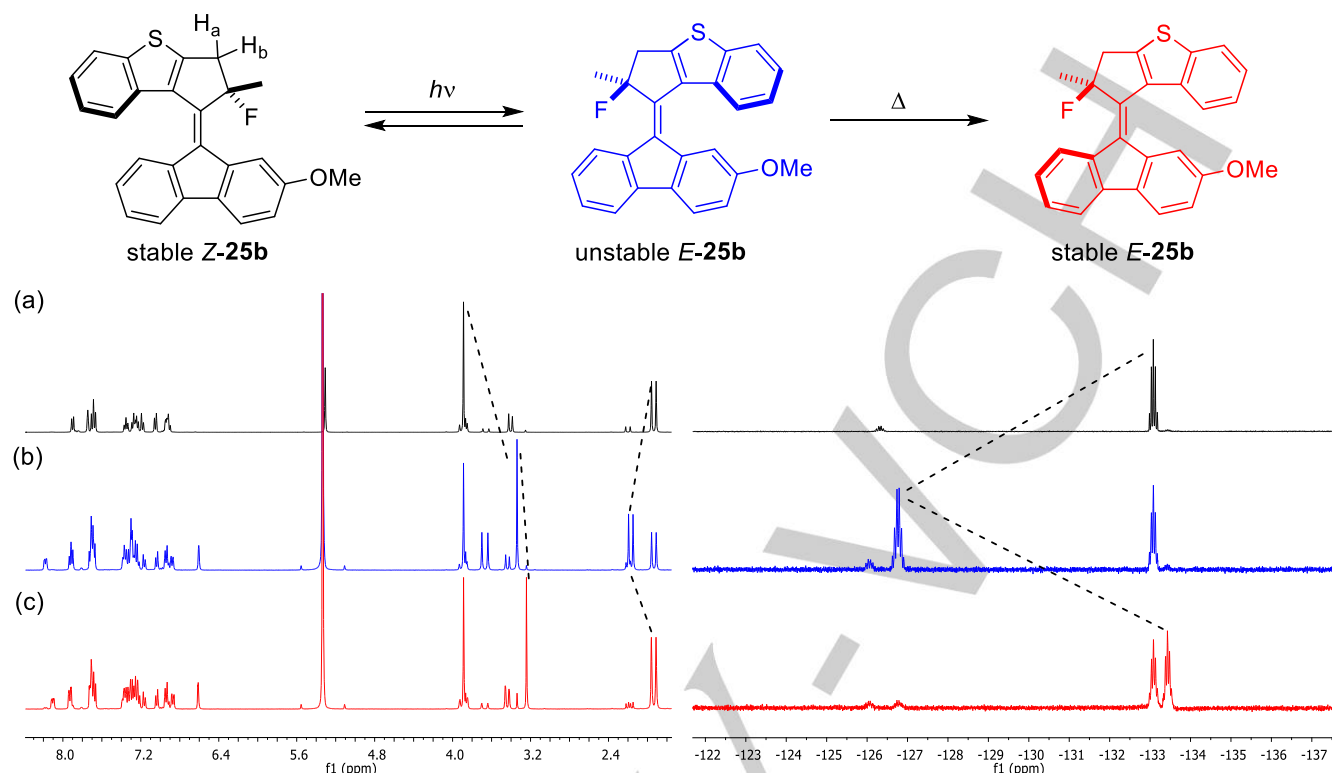


Figure 5. ^1H and ^{19}F NMR spectroscopy (400 MHz, CD_2Cl_2 , 233 K, $c = \sim 1 \times 10^{-2}$ M). (a) ^1H NMR (left) and ^{19}F NMR (right) of the stable **Z-25b**. (b) irradiation (365 nm) to PSS at 233 K and formation of the corresponding unstable **E-25b**; the mixture consists of stable **Z-25b** (38%), stable **E-25b** (4%), unstable **E-25b** (50%) and unstable **Z-25b** (8%). (c) after heating to 293 K for 16 h. formation of stable **E-25b** is observed, confirming that thermal helix inversion is taking place.

The UV-vis absorption spectra of **25a** in heptane at 273 K shows an absorption band centered at 375 nm (Figure 3c, solid black). Irradiation of the samples with UV light (365 nm) at 273 K gave rise to a bathochromically shifted absorption band at 394 nm, indicating the formation of the unstable diastereoisomer (Figure 3c, blue solid). A single isosbestic point was observed throughout the irradiation. After the photostationary state (PSS) was reached, the sample was warmed to 293 K for 30 min and full reversal to the original UV-vis spectra was observed, indicating that either the anticipated thermal helix inversion or possibly the thermal backward *E-Z* isomerization is taking place (Figure 3c, red dashed). Eyring analysis of the thermal step was performed using a procedure identical to compounds **5a-b** and **6**. The Gibbs free energy of activation $\Delta^\ddagger G^\circ$ for thermal isomerization of the unstable **25a** back to the stable **25a** was found to be $88.4 \pm 0.0 \text{ kJ} \cdot \text{mol}^{-1}$ ($\Delta^\ddagger H^\circ$ $65.1 \pm 0.2 \text{ kJ} \cdot \text{mol}^{-1}$, $\Delta^\ddagger S^\circ$ $-79.5 \pm 0.5 \text{ J} \cdot \text{K}^{-1} \cdot \text{mol}^{-1}$), corresponding to a half-life of $642 \pm 1 \text{ s}$ at room temperature (Table 2). Just like in the previous cases, the observed value for the thermal step is much higher than that reported for the desfluoro parent compound ($\Delta^\ddagger G^\circ = 71.1 \text{ kJ} \cdot \text{mol}^{-1}$, $t_{1/2}(298 \text{ K}) = 520 \text{ ms}$).^[47]

While such a low barrier ($\Delta^\ddagger G^\circ < 100 \text{ kJ} \cdot \text{mol}^{-1}$) has not been observed for a thermal *E-Z* isomerization before, it was necessary to exclude this possibility and assess the nature of the thermal step by ^1H and ^{19}F NMR spectroscopy of the desymmetrized motor **25b**. A sample of **Z-25b** in CD_2Cl_2 (Figure 5a) was thus prepared. Interestingly, a minor amount ($\sim 10\%$) of the unstable **Z-25b** (additional methyl resonance at 2.21 ppm and fluorine resonance at -126.1 ppm) was present in the sample prior to irradiation and after extensive heating, furthermore, the ratio was found to be dependent on

temperature. This is due to a relatively small difference in energy between the stable **Z-25b** and its corresponding unstable **Z-25b** ($< 10 \text{ kJ} \cdot \text{mol}^{-1}$) as confirmed by computations (*vide infra*).

Irradiation of the sample with UV-light (365 nm) at 233 K resulted in the appearance of unstable **E-25b** according to both ^1H and ^{19}F NMR spectroscopy (Figure 5b). The most significant change that occurred was a shift of the methoxy group resonance from 3.89 ppm to 3.34 ppm as a consequence of the photochemical *E-Z* isomerization of stable **Z-25b** to unstable **E-25b**. In the region of the resonance of the stereogenic methyl group of unstable **Z-25b** ($\sim 2.20 \text{ ppm}$), an additional methyl resonance at $\sim 2.35 \text{ ppm}$ appeared, reinforcing the fact that the minor compound observed in the initial sample is indeed unstable **Z-25b**. A downfield shift of $\text{H}_{a/b}$ from 3.40 ppm to 3.67 ppm was also observed (Figure 5b, left). Likewise, in addition to the two original resonances in the ^{19}F NMR spectrum at -133.1 ppm (major, stable **Z-25b**) and -126.1 ppm (minor, unstable **Z-25b**), an additional absorption at -126.8 ppm emerged upon irradiation due to formation of unstable **E-25b** (Figure 5b, right). When the PSS was reached, the mixture consisted of stable **Z-25b** (38%), stable **E-25b** (4%), unstable **E-25b** (50%) and unstable **Z-25b** (8%) as determined by integration of the resonances in ^{19}F NMR spectrum. The sample was then heated to 293 K for 30 min and ^1H and ^{19}F NMR spectrum were recorded again (Figure 5c, left and right respectively). After performing the thermal step, the mixture consisted of stable **Z-25b** (46%) and **E-25b** (54%) and residual amounts of the unstable forms (see ratios before). These data unequivocally demonstrate that the barrier for THI is lower than for the backward thermal *E-Z* isomerization, facilitating the ability

of **25a-b** to functional as photochemically driven unidirectional molecular motors.

Computational results

The experimental study of the thermal behavior of the unstable diastereoisomers (**5**, **6** and **25a**) of the fluorinated motors was supplemented with a computational investigation using DFT calculations. Initial geometries were optimized using the semi-empirical PM3 method after which the thermal helix inversion was studied by scanning dihedral angles governing the aromatic planes (indicated by bold bonds in the structures in Figure 6) using the same method. The minima and transition states were further optimized by DFT (B3LYP/6-31G(d,p)) and a frequency analysis confirmed the identity of each geometry as well as providing their thermochemistry.

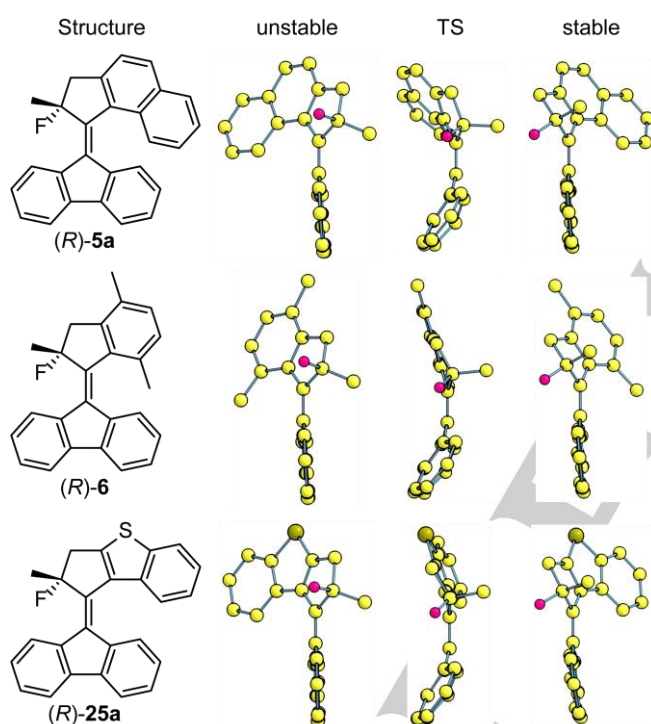


Figure 6. Quaternarized second generation molecular motors **5a**, **6** and **25a**. Side-view of the calculated geometries (DFT B3LYP/6-31G(d,p)) of the unstable and stable diastereoisomers as well as the transition state (TS).

The calculated geometries of **5a**, **6** and **25a** are shown in Figure 6, exhibiting a large consistency in configuration between the different molecules. The global minimum, i.e. the stable isomer, for all quaternarized motors is found to orient the fluorine at the stereogenic center pseudo-equatorially towards the lower half analogous to the orientation of the stereogenic hydrogen in common second generation molecular motors.^[46] In the same way were all local minima, i.e. the unstable isomers, found to orient the stereogenic fluorine pseudo-axially. The unstable states of the studied motors (**5a**, **6** and **25a**) were all connected to the corresponding stable state by a transition state constituting a thermal helix inversion pathway. The calculated

thermochemistry (Table 3) shows the barrier for THI to follow the same trend as the parent desfluoro analogues, however, the individual barriers of the motors **5a**, **6** and **25a** are significantly higher (Table 2). The barriers for the motors **5a** and **6** are of such magnitude that high temperatures would be required to bring about their THI, thus allowing backward thermal *E-Z* isomerization to become a competing process. The increase in energy is caused by additional steric hindrance of the fluorine atom with the lower half. While the major part of the barrier stems from the hindrance of the moieties in the fjord region, the smallest substituent on the stereogenic center comes into close proximity of the lower half as well (see TS's in Figure 6). The result is that the lower halves of the transition states require a larger degree of folding than their hydrogen substituted analogues. These results are consistent with the experimental observations made for **5a** and **6**, for which a considerable increase (>20 kJ·mol⁻¹) of the THI barrier has been found, resulting in thermal backward *E-Z* isomerization being the major process (Table 2, Figure 4). At the same time, the calculated barrier for THI of **25a** (88.9 kJ·mol⁻¹, Table 3) is in a perfect agreement with the experimentally obtained value of 88.4 kJ·mol⁻¹ (Table 2) and the observed forward thermal helix inversion pathway

Table 3. Calculated thermochemistry of motors **5a**, **6** and **25a** (DFT B3LYP/6-31G(d,p)).

Motor	5a	6	25a
ΔG° unstable ^[a] [kJ·mol ⁻¹]	8.7	9.5	4.3
unstable [%] ^[b]	2.8	2.0	15
ΔG° TS [kJ·mol ⁻¹]	133	127	93.2
$\Delta^\ddagger G^\circ$ TS [kJ·mol ⁻¹]	124	118	88.9

[a] Energy difference between the stable and the corresponding unstable state
[b] Boltzmann population of the unstable state at rt.

Due to the fluorine atom replacing the stereogenic hydrogen, the difference in Gibbs energy between the stable and unstable configurations of **25a-b** has decreased, leading to a measurable population (15% by DFT, Table 3) of the unstable **25a** state under equilibrium conditions, as has been observed experimentally by both ¹H and ¹⁹F NMR spectroscopy for unstable *Z*-**25b** (~10%, Figure 5). The drop in the difference in energy agrees well with the reduction in the difference in substituent size on the stereogenic center, and suggests that a population of the unstable configuration can be reduced by, for example, a replacement of the methyl group by a *tert*-butyl group.

Conclusions

A series of fluorinated second generation motor analogues (**4**, **5a-b**, **6** and **25a-b**) with a quaternary stereogenic center have been synthesized. A major increase (20–25 kJ·mol⁻¹) in the barrier for thermal isomerization compared to the parent compounds has been observed for all the cases, presumably due to destabilization of the transition state in which the fluorine is forced to pass around the lower half. Being larger in size than the original hydrogen, the steric penalty imposed on the molecule is larger, leading to an increase in energy for the

transition state. It has been experimentally demonstrated (and supported by calculations), that a motor with a sufficiently low barrier for THI (**25a-b**) can still function as a proper unidirectional photochemically driven molecular motor upon fluorination. This modification opens additional avenues in tuning the speed and stability of the molecular motors leading to new potential applications.

Experimental Section

2-Methyl-3-(naphthalen-2-ylthio)propanoic acid (**7**).

Methacrylic acid (4.2 ml, 50.0 mmol) was added slowly to a stirred solution of naphthalene-2-thiol (4.0 g, 25.0 mmol) and triethylamine (6.96 ml, 50.0 mmol) in THF (50 ml) at room temperature. The resulting mixture was heated to reflux for 16 h. Subsequently, it was quenched with aq. HCl (1 M) until the mixture was acidic (pH = 2). The mixture was extracted with ethyl acetate (3 × 50 ml). The combined organic extracts were washed with brine (50 ml), dried over MgSO₄ and the solvents evaporated at reduced pressure. The residue was recrystallized from heptane (~40 ml) to give the product **7**. Yield: 4.86 g (79%). Tan solid. Mp 89.3–90.5 °C. ¹H NMR (400 MHz, CDCl₃): δ (ppm) 10.3 (brs, 1H), 7.78–7.85 (m, 4H), 7.44–7.52 (m, 3H), 3.41 (ddd, *J* = 13.4, 6.8, 1.8 Hz, 1H), 3.04 (ddd, *J* = 13.4, 7.0, 1.5 Hz, 1H), 2.78 (m, 1H), 1.45 (dd, *J* = 7.0, 1.5 Hz, 3H). ¹³C NMR (100 MHz, CDCl₃): δ (ppm) 181.6, 133.9, 133.0, 132.2, 128.8, 128.5, 128.1, 127.9, 127.4, 126.8, 126.1, 39.8, 37.1, 16.7.

2-Methyl-2,3-dihydro-1*H*-benzo[*f*]thiochromen-1-one (**8**).

Oxalyl chloride (2.83 ml, 32.3 mmol) was added dropwise to a solution of **7** (5.3 g, 21.5 mmol) and three drops of DMF in dry CH₂Cl₂ (80 ml) at room temperature under N₂ atmosphere. After stirring for 1 h, the volatiles were evaporated at reduced pressure and the residue was redissolved in dry CH₂Cl₂ (80 ml). The solution was cooled to –10 °C and solid AlCl₃ was added portionwise over 10 min. The mixture was stirred for additional 2 h at –10 °C and then quenched by pouring into ice cold aq. HCl (1 M, 100 ml). The mixture was extracted with CH₂Cl₂ (3 × 80 ml). The combined organic extracts were washed with brine (50 ml), dried over MgSO₄ and the solvents evaporated at reduced pressure. The residue was purified by column chromatography on silica gel (pentane : ethyl acetate – 50 : 1) to provide the title product **8**. Yield: 4.86 g (86%). Pale yellow oil. ¹H NMR (400 MHz, CDCl₃): δ (ppm) 9.07 (d, *J* = 8.7 Hz, 1H), 7.75 (dd, *J* = 7.7, 7.7 Hz, 2H), 7.59 (dd, *J* = 7.7, 7.7 Hz, 1H), 7.44 (dd, *J* = 7.4, 7.4 Hz, 1H), 7.23 (d, *J* = 8.7 Hz, 1H), 3.07–3.28 (m, 3H), 1.40 (d, *J* = 6.4 Hz, 3H). ¹³C NMR (100 MHz, CDCl₃): δ (ppm) 199.1, 143.9, 133.0, 132.3, 131.5, 128.8, 128.2, 125.6, 125.4, 125.1, 124.9, 42.7, 32.5, 15.2.

2-Fluoro-2-methyl-2,3-dihydro-1*H*-benzo[*f*]thiochromen-1-one (**9**).

A solution of **8** (1.0 g, 4.38 mmol) in dry toluene (10 ml) was added to a solution of NaHMDS (2.85 ml, 5.69 mmol, 2 M in THF) in dry toluene (50 ml) at –78 °C under N₂ atmosphere. After stirring for 30 min at this temperature, NFSI (2.07 g, 6.57 mmol) was added portionwise over 10 min. The reaction mixture was allowed to spontaneously warm up to room temperature overnight. The reaction was quenched by addition of aq. HCl (1 M, 60 ml). The mixture was extracted with CH₂Cl₂ (3 × 50 ml), the combined organic extracts were washed with brine (50 ml) and dried over MgSO₄. The solvents evaporated at reduced pressure and the residue was purified by column chromatography on silica gel (pentane : ethyl acetate – 50 : 1) to afford the desired product. Yield: 723 mg (67%). Yellow oil. ¹H NMR (400 MHz, CDCl₃): δ (ppm) 9.10 (d, *J* = 8.8 Hz, 1H), 7.82

(d, *J* = 8.7 Hz, 1H), 7.77 (d, *J* = 8.1 Hz, 1H), 7.64 (dd, *J* = 7.8, 7.8 Hz, 1H), 7.49 (dd, *J* = 7.4, 7.4 Hz, 1H), 7.21 (d, *J* = 8.7 Hz, 1H), 3.74 (dd, *J* = 13.1, 7.9 Hz, 1H), 3.25 (dd, *J* = 12.4, 12.7 Hz, 1H), 1.82 (d, *J* = 21.5 Hz, 3H). ¹³C NMR (100 MHz, CDCl₃): δ (ppm) 193.3 (d, *J* = 19.0 Hz), 143.1, 134.5, 132.9, 131.7, 129.7, 128.7, 126.2, 125.4, 124.5, 123.6, 91.9 (d, *J* = 186.3 Hz), 35.5 (d, *J* = 28.1 Hz), 20.9 (d, *J* = 25.1 Hz). ¹⁹F NMR (376 MHz, CDCl₃): δ (ppm) –149.6. HRMS (APCI⁺): calcd for C₁₄H₁₂FOS (M + H⁺) 247.0587 found 247.0589.

Note: Use of THF as a solvent instead of toluene drastically decreases the yield of the desired product (<10%) due to formation of 2-methyl-1*H*-benzo[*f*]thiochromen-1-one as the major product.

2-Fluoro-2-methyl-1-(9*H*-thioxanthen-9-ylidene)-2,3-dihydro-1*H*-benzo[*f*]thiochromene (**4**).

A mixture of **9** (320 mg, 1.30 mmol), P₄S₁₀ (866 mg, 3.90 mmol) and Lawesson's reagent (1.58 g, 3.9 mmol) in toluene (20 ml) was heated at reflux for 3 h. The mixture was allowed to cool down to room temperature and was directly purified by column chromatography on silica gel (pentane : ethyl acetate – 20 : 1). The fractions containing the thioketone were concentrated under reduced pressure to a small volume. In the meantime, a stirred solution of (9*H*-thioxanthen-9-ylidene)hydrazine^[49] (552 mg, 2.44 mmol) in anhydrous THF (30 ml) was treated with MnO₂ (1.06 g, 12.2 mmol) at 0 °C. After 30 min, the suspension was filtered through a short plug of Celite. The pad was washed with a small amount of anhydrous THF and the combined filtrates cooled back to 0 °C. To this solution, the aforementioned thioketone in small amount of solvents was added dropwise. The resulting mixture was left stirring overnight after which the solvents were evaporated at reduced pressure. The residue was redissolved in toluene (10 ml), HMPT (222 μl, 1.22 mmol) was added and the mixture was heated to 50 °C overnight. The crude reaction mixture was adsorbed on Celite and purified by column chromatography (pentane : CH₂Cl₂ – 15 : 1). (Note: The compound slowly oxidizes on silica gel, therefore the purification should be performed swiftly.) The pale yellow solid afforded thereafter was further purified by washing with cold pentane (3 × 2 ml) to give the pure final compound **4**. Yield: 87 mg (17%). White solid. Mp 150–152 °C (dec.). ¹H NMR (400 MHz, CDCl₃): δ (ppm) 7.78 (dd, 1H, *J*₁ = 8.4 Hz, *J*₂ = 8.3 Hz), 7.66 (d, 1H, *J* = 8.4 Hz), 7.61 (d, 1H, *J* = 8.5 Hz), 7.58 (dd, 2H, *J*₁ = 7.5 Hz, *J*₂ = 7.5 Hz), 7.44 (d, 1H, *J* = 8.5 Hz), 7.22–7.31 (m, 3H), 7.16 (dd, 1H, *J*₁ = 7.2 Hz, *J*₂ = 7.2 Hz), 7.08 (dd, 1H, *J*₁ = 7.5 Hz, *J*₂ = 7.5 Hz), 6.67 (dd, 1H, *J*₁ = 7.5 Hz, *J*₂ = 7.4 Hz), 6.37 (dd, 1H, *J*₁ = 7.5 Hz, *J*₂ = 7.5 Hz), 6.31 (d, 1H, *J* = 7.6 Hz), 3.68 (dd, 1H, *J*₁ = 23.1 Hz, *J*₂ = 12.2 Hz), 3.29 (dd, 1H, *J*₁ = 12.7 Hz, *J*₂ = 12.7 Hz), 1.35 (d, 3H, *J* = 21.5 Hz). ¹³C NMR (100 MHz, CDCl₃): δ (ppm) 139.3, 136.4, 136.4, 135.9, 135.3, 135.1, 134.4, 134.4, 134.2, 134.2, 134.1, 131.9, 131.0, 131.0, 131.0, 130.8, 128.6, 128.1, 127.7, 127.3, 127.3, 126.8, 126.7, 126.4, 126.0, 125.7, 125.3, 125.3, 125.3, 125.1, 124.6, 99.7 (d, *J* = 194.3 Hz), 43.0 (d, *J* = 26.6 Hz), 27.1 (d, *J* = 28.1 Hz). ¹⁹F NMR (376 MHz, CDCl₃): δ (ppm) –127.9 (m). HRMS (ESI): calcd for C₂₇H₂₀FS₂ [M + H⁺] 427.0985 found 427.0983.

2-Methyl-2,3-dihydro-1*H*-cyclopenta[*a*]naphthalen-1-one (**14**)

A mixture of AlCl₃ (10.4 g, 78 mmol) and methacryloyl chloride (3.8 ml, 39 mmol) in dry CH₂Cl₂ (100 ml) was cooled down to –78 °C. Solid naphthalene was added portionwise to this mixture over 10 min. The mixture was allowed to attain room temperature overnight. The solution was then poured onto a mixture of ice (~100 g) and aq. HCl (1 M, 50 ml). The resulting mixture was extracted with diethyl ether (3 × 70 ml). The combined organic extracts were washed with brine (50 ml), dried over MgSO₄ and the solvents evaporated at reduced pressure. The crude product was purified by column chromatography on

silica gel (pentane : ethyl acetate – 50 : 1) to provide the product **14**. Yield: 4.71 g (62%). Pale yellow oil. ¹H NMR (400 MHz, CDCl₃): δ (ppm) 9.17 (d, *J* = 8.3 Hz, 1H), 8.03 (d, *J* = 8.4 Hz, 1H), 7.89 (d, *J* = 8.1 Hz, 1H), 7.67 (dd, *J* = 8.2, 7.1 Hz, 1H), 7.56 (dd, *J* = 8.1, 7.0 Hz, 1H), 7.49 (d, *J* = 8.4 Hz, 1H), 3.47 (dd, *J* = 18.1, 8.1 Hz, 1H), 2.78–2.86 (m, 2H), 1.39 (d, *J* = 7.3 Hz, 3H). ¹³C NMR (100 MHz, CDCl₃): δ (ppm) 209.1, 156.1, 135.1, 132.2, 129.5, 129.0, 128.2, 127.6, 126.1, 123.44, 123.39, 41.8, 34.7, 16.2.

2-Fluoro-2-methyl-2,3-dihydro-1*H*-cyclopenta[*a*]naphthalen-1-one (**16**).

A solution of LiHMDS (6.6 ml, 6.6 mmol, 1 M in THF) in anhydrous toluene (40 ml) was cooled down to –78 °C. A solution of **14** (1.0 g, 5.1 mmol) in anhydrous toluene (5 ml) was added dropwise. After stirring for 30 min, NFSI (2.25 g, 7.1 mmol) was added portionwise. The resulting mixture was allowed to spontaneously warm up to ambient temperature overnight. The reaction was quenched by addition of aq. HCl (1 M, 60 ml). The mixture was extracted with CH₂Cl₂ (3 × 50 ml), the combined organic extracts were washed with brine (50 ml) and dried over MgSO₄. The solvents were evaporated at reduced pressure and the crude product was purified by column chromatography on silica gel (pentane : ethyl acetate – 15 : 1) to provide the product as pale yellow oil (908 mg, 83%). ¹H NMR (400 MHz, CDCl₃): δ (ppm) 9.05 (d, *J* = 8.3 Hz, 1H), 8.08 (dd, *J* = 8.3, 4.8 Hz, 1H), 7.88 (m, 1H), 7.69 (m, 1H), 7.57 (m, 1H), 7.44 (m, 1H), 3.33–3.59 (m, 2H), 1.69 (d, *J* = 22.8 Hz, 3H). ¹³C NMR (100 MHz, CDCl₃): δ (ppm) 201.5 (d, *J* = 18.9 Hz), 153.4 (d, *J* = 4.4 Hz), 137.5, 133.0, 129.7, 129.6, 128.5, 127.9, 127.2, 124.2, 123.7, 95.8 (d, *J* = 183.9 Hz), 41.0 (d, *J* = 24.7 Hz), 22.0 (d, *J* = 26.8 Hz). ¹⁹F NMR (376 MHz, CDCl₃): δ (ppm) –151.2. HRMS (ESI): calcd for C₁₄H₁₂FO [M + H⁺] 215.0867 found 215.0863.

9-(2-Fluoro-2-methyl-2,3-dihydro-1*H*-cyclopenta[*a*]naphthalen-1-ylidene)-9*H*-fluorene (**5a**).

A mixture of **16** (300 mg, 1.4 mmol), P₄S₁₀ (467 mg, 2.1 mmol), Lawesson's reagent (850 mg, 2.1 mmol) in toluene (20 ml) was heated at reflux for 1 h. The dark green mixture was concentrated under reduced pressure and purified directly on a short column of silica gel (pentane : ethyl acetate – 15 : 1) to give a dark green oil. The oil was redissolved in toluene (20 ml) and 9-diazo-9*H*-fluorene^[38] (377 mg, 1.96 mmol) was added portionwise over 5 min. The resulting mixture was left stirring overnight and HMPT (514 μl, 457 mg, 2.8 mmol) was added afterwards. The mixture was stirred for additional 24 h at room temperature. The crude reaction mixture (adsorbed on Celite) was purified by column chromatography on silica gel (pentane : ethyl acetate – 50 : 1), followed by crystallization from ethanol (10 mL) to give the motor **5a** as a yellow solid (247 mg, 0.68 mmol, 49%). Mp. (dec.) >210 °C. ¹H NMR (400 MHz, CDCl₃): δ (ppm) 8.23 (m, 1H), 7.94 (dd, *J* = 9.0 Hz, 2H), 7.85–7.79 (m, 1H), 7.75 (d, *J* = 7.5 Hz, 1H), 7.70 (d, *J* = 8.5 Hz, 1H), 7.52 (d, *J* = 8.2 Hz, 1H), 7.47 (dd, *J* = 7.4 Hz, 1H), 7.44–7.36 (m, 2H), 7.33–7.20 (m, 2H), 6.77 (dd, *J* = 7.4 Hz, 1H), 6.72 (d, *J* = 7.8 Hz, 1H), 3.92 (dd, 1H, *J* = 16.2 Hz), 3.30 (d, 1H, *J* = 14.5 Hz), 1.93 (d, 3H, *J* = 19.1 Hz). ¹³C NMR (100 MHz, CDCl₃): δ (ppm) 144.9, 144.7, 143.3, 143.2, 140.9, 140.4, 138.3, 137.9, 134.9, 133.0, 132.2, 131.9, 129.3, 129.1, 127.9, 127.7, 127.3, 127.2, 126.9, 126.2, 125.9, 125.9, 123.2, 123.2, 119.5, 119.1, 106.8, 105.8 (d, *J* = 195.5 Hz), 48.7 (d, *J* = 24.3 Hz), 23.8 (d, *J* = 25.7 Hz). ¹⁹F NMR (376 MHz, CDCl₃): δ (ppm) –138.94 (pd, *J* = 19.0, 4.4 Hz). HRMS (ESI): calcd for C₂₇H₂₀ [M – F⁻] 343.1481 found 343.1488.

(*E*)-9-(2-fluoro-2-methyl-2,3-dihydro-1*H*-cyclopenta[*a*]naphthalen-1-ylidene)-2-methoxy-9*H*-fluorene (**5b**).

A mixture of **16** (301 mg, 1.4 mmol), P₄S₁₀ (623 mg, 2.8 mmol), Lawesson's reagent (1.13 g, 2.8 mmol) in toluene (20 ml) was heated at reflux for 1 h. The dark green mixture was concentrated under reduced pressure to ~5 ml and purified directly on a short column of silica gel (pentane : ethyl acetate – 20 : 1) to give a dark green oil. In the meanwhile, (2-methoxy-9*H*-fluorene-9-ylidene)hydrazine^[38] (408 mg, 1.8 mmol) was dissolved in THF (30 ml) and cooled down to 0 °C. MnO₂ (1.22 g, 14.0 mmol) was added to the vigorously stirred solution. After stirring for 30 min, the suspension was filtered through a short plug of silica gel. The pad was washed with a small amount of THF and the combined filtrates cooled back to 0 °C. To this solution, the aforementioned thioetone in a small amount of solvent was added dropwise. The resulting mixture was left stirring overnight and HMPT (514 μl, 2.8 mmol) was added afterwards. The mixture was stirred for additional 24 h at room temperature. The crude reaction mixture was adsorbed on Celite Purification by column chromatography on silica gel (pentane : ethyl acetate – 50 : 1), followed by two crystallizations from heptane (~10 ml) afforded the product as a mixture of *EZ* isomers in 33:1 ratio. Yield: 135 mg (25%). Orange solid. Mp. (dec.) >210 °C. ¹H NMR (400 MHz, CDCl₃): δ (ppm) 8.20–8.11 (m, 1H), 7.92 (dd, *J* = 7.9 Hz, 2H), 7.70 (m, 2H), 7.59 (d, *J* = 8.2 Hz, 1H), 7.52 (d, *J* = 8.2 Hz, 1H), 7.46 (dd, *J* = 7.4 Hz, 1H), 7.32 (m, 3H), 6.79 (d, *J* = 8.0 Hz, 1H), 6.23 (s, 1H), 3.91 (dd, *J* = 15.8 Hz, 1H), 3.31 (d, *J* = 14.7 Hz, 1H), 2.92 (s, 3H), 1.96 (d, *J* = 19.2 Hz, 3H). ¹³C NMR (100 MHz, CDCl₃): δ (ppm) 158.5, 144.8, 144.6, 143.4, 143.3, 141.1, 139.1, 138.1, 134.8, 134.7, 133.8, 133.0, 132.4, 131.9, 129.2, 129.1, 127.8, 127.7, 127.3, 127.3, 127.1, 125.8, 125.8, 123.3, 123.3, 119.8, 118.8, 115.9, 110.3, 105.7 (d, *J* = 195.4 Hz), 48.7 (d, *J* = 24.5 Hz), 23.8 (d, *J* = 25.7 Hz). ¹⁹F NMR (376 MHz, CDCl₃): δ (ppm) –138.7 (m) (*Z*-isomer), –139.14 (pd, *J* = 19.0, 3.9 Hz) (*E*-isomer). HRMS (ESI): calcd for C₂₈H₂₁O [M – F⁻] 373.1587 found 373.1599.

2-Fluoro-2,4,7-trimethyl-2,3-dihydro-1*H*-inden-1-one (**15**).

A solution of LiHMDS (3.7 ml, 7.5 mmol, 2 M in THF) in anhydrous toluene (40 ml) was cooled down to –78 °C. A solution of 2,4,7-trimethyl-2,3-dihydro-1*H*-inden-1-one (1.00 g, 5.7 mmol) in anhydrous toluene (5 ml) was added dropwise. After stirring at –78 °C for 30 min, NFSI (2.35 g, 7.5 mmol) was added portionwise. The resulting mixture was allowed to spontaneously warm up to ambient temperature overnight. The reaction was quenched by addition of aq. HCl (1 M, 60 ml). The mixture was extracted with CH₂Cl₂ (3 × 50 ml), the combined organic extracts were washed with brine (50 ml) and dried over MgSO₄. The solvents were evaporated at reduced pressure and the crude product was purified by column chromatography on silica gel (pentane : ethyl acetate – 20 : 1) to provide the product as a pale yellow oil (943 mg, 4.9 mmol, 85%). ¹H NMR (400 MHz, CDCl₃): δ (ppm) 7.28 (d, *J* = 7.5 Hz, 1H), 7.04 (d, *J* = 7.5 Hz, 1H), 3.29–3.04 (m, 2H), 2.57 (s, 3H), 2.25 (s, 3H), 1.58 (d, *J* = 22.8 Hz, 3H). ¹³C NMR (100 MHz, CDCl₃): δ (ppm) 202.2 (d, *J* = 18.2 Hz), 149.4 (d, *J* = 3.9 Hz), 137.4, 136.1, 132.9, 130.9, 130.1, 95.56 (d, *J* = 183.0 Hz), 39.0 (d, *J* = 24.5 Hz), 21.9 (d, *J* = 26.8 Hz), 17.8 (d, *J* = 57.0 Hz). ¹⁹F NMR (376 MHz, CDCl₃): δ (ppm) –150.5 (m). HRMS (ESI): calcd for C₁₂H₁₄FO (M + H⁺) 193.1029 found 193.1026.

9-(2-Fluoro-2,4,7-trimethyl-2,3-dihydro-1*H*-inden-1-ylidene)-9*H*-fluorene (**6**).

A mixture of **15** (358 mg, 1.9 mmol), P₄S₁₀ (623 mg, 2.8 mmol), Lawesson's reagent (1.13 g, 2.8 mmol) in toluene (20 ml) was heated at reflux for 1 h. The dark green mixture was concentrated under reduced pressure and purified directly on a short column of silica gel (pentane : ethyl acetate – 20 : 1) to give a dark green oil. The oil was redissolved in toluene (20 ml) and 9-diazo-9*H*-fluorene (501 mg, 2.6 mmol) was added

portionwise over 5 min. The resulting mixture was left stirring overnight and HMPT (683 μ l, 608 mg, 3.7 mmol) was added afterwards. The mixture was stirred for additional 24 h at room temperature. The crude reaction mixture was purified by column chromatography on silica gel (pentane : ethyl acetate – 50 : 1), trituration by hot methanol (2 \times 7 mL) and recrystallization from ethanol (20 mL) to provide **6** as a yellow solid (319 mg, 0.94 mmol, 50%). Mp. (dec.) >210 °C. ¹H NMR (400 MHz, CDCl₃): δ (ppm) 8.17 (m, 1H), 7.86–7.72 (m, 2H), 7.37 (m, 4H), 7.22–7.07 (m, 3H), 3.69–3.52 (dd, J = 16.1 Hz, 1H), 3.18 (d, J = 14.5 Hz, 1H), 2.36 (s, 3H), 2.20 (s, 2H), 1.93 (d, J = 19.3 Hz, 3H). ¹³C NMR (100 MHz, CDCl₃): δ (ppm) 146.2, 146.0, 141.5, 141.4, 140.6, 140.4, 138.7, 138.2, 135.0, 132.0, 131.2, 131.0, 129.8, 128.0, 127.6, 127.2, 127.1, 126.8, 123.8, 119.5, 119.3, 105.1 (d, J = 194.2 Hz), 46.6 (d, J = 24.0 Hz), 23.7 (d, J = 25.9 Hz), 21.4, 18.4. ¹⁹F NMR (376 MHz, CDCl₃): δ (ppm) –139.9 (pd, J = 19.0, 4.4 Hz). HRMS (ESI): calcd for C₂₆H₂₃ [M – F] 351.1743 found 351.1752.

2-Fluoro-2-methyl-2,3-dihydro-1H-benzo[b]cyclopenta[d]thiophen-1-one (**22**).

A solution of LiHMDS (1.38 ml, 1.4 mmol, 1 M in THF) in anhydrous toluene (40 ml) was cooled down to –78 °C. 2-Methyl-2,3-dihydro-1H-benzo[b]cyclopenta[d]thiophen-1-one^[50] (200 mg, 0.99 mmol) in anhydrous toluene (5 ml) was added dropwise to this solution. After stirring at –78 °C for 30 min, NFSI (468 mg, 1.5 mmol) was added portionwise. The resulting mixture was allowed to spontaneously warm up to ambient temperature overnight. The reaction was quenched by addition of aq. HCl (1 M, 60 ml). The mixture was extracted with CH₂Cl₂ (3 \times 50 ml), the combined organic extracts were washed with brine (50 ml) and dried over MgSO₄. The solvents were evaporated at reduced pressure and the crude product was purified by column chromatography on silica gel (pentane : ethyl acetate – 30 : 1) to provide **22** as pale yellow oil (83 mg, 0.38 mmol 38%). ¹H NMR (400 MHz, CDCl₃): δ (ppm) 8.22 (d, J = 7.5 Hz, 1H), 7.82 (d, J = 8.0 Hz, 1H), 7.47 (ddd, J = 7.8, 7.6, 1.1 Hz, 1H), 7.41 (ddd, J = 7.8, 7.6, 1.1 Hz, 1H), 3.68 – 3.32 (m, 2H), 1.70 (d, J = 23.0 Hz, 3H). ¹³C NMR (100 MHz, CDCl₃): δ (ppm) 192.2 (d, J = 19.6 Hz), 170.2 (d, J = 5.2 Hz), 143.8, 136.2, 131.4, 126.3, 126.2, 123.4, 123.1, 99.5 (d, J = 189.5 Hz), 39.8 (d, J = 27.0 Hz), 21.8 (d, J = 26.3 Hz). ¹⁹F NMR (376 MHz, CDCl₃): δ (ppm) –146.2 (qdd, J = 23.0, 19.6, 10.0 Hz). HRMS (ESI): calcd for C₁₂H₁₀FOS [M + H⁺] 221.0436 found 221.0447.

1-(9H-Fluoren-9-ylidene)-2-fluoro-2-methyl-2,3-dihydro-1H-benzo[b]cyclopenta[d]thiophene (**25a**).

A mixture of **22** (100 mg, 0.45 mmol), P₄S₁₀ (151 mg, 0.68 mmol), Lawesson's reagent (275 mg, 0.68 mmol) in toluene (10 ml) was heated to 100 °C for 1 h. After TLC showed no remaining starting material, the dark green mixture was concentrated under reduced pressure and purified directly on a short column of silica gel (pentane : ethyl acetate – 20 : 1) to give a dark green oil. The oil was redissolved in toluene (20 ml) and 9-diazo-9H-fluorene^[38] (122 mg, 0.64 mmol) was added portionwise over 5 min. The resulting mixture was left stirring overnight and HMPT (167 μ l, 148 mg, 0.91 mmol) was added afterwards. The mixture was stirred for an additional 24 h at room temperature. The crude reaction mixture was purified by column chromatography on silica gel (pentane : CH₂Cl₂ – 7 : 1) and recrystallization from ethanol to give the motor **25a** as a yellow solid (102 mg, 0.28 mmol, 61%). Mp. (dec.) >200 °C. ¹H NMR (400 MHz, CDCl₃): δ (ppm) 8.20 (d, J = 5.0 Hz, 1H), 7.92 (d, J = 8.1 Hz, 1H), 7.83 (m, 2H), 7.42–7.31 (m, 4H), 7.27 (dd, J = 7.6 Hz, 1H), 7.21 (d, J = 7.8 Hz, 1H), 7.14 (d, J = 7.8 Hz, 1H), 7.02 (dd, J = 7.4 Hz, 1H), 3.91 (dd, J = 15.6 Hz, 1H), 3.42 (d, J = 15.1 Hz, 1H), 1.96 (d, J = 19.0 Hz, 3H). ¹³C NMR (100 MHz, CDCl₃): δ (ppm) 152.3 (d, J = 12.0 Hz), 152.2, 143.9, 140.9,

140.4, 138.5, 138.3, 133.9, 128.9, 128.0, 127.7, 127.2, 127.2, 127.1, 127.0, 126.9, 126.6, 126.4, 124.9, 124.87, 123.8, 120.0, 119.5, 108.2 (d, J = 198.6 Hz), 46.1 (d, J = 26.9 Hz), 24.1 (d, J = 25.1 Hz). ¹⁹F NMR (376 MHz, CDCl₃): δ (ppm) –132.9 (m). HRMS (ESI): calcd for C₂₅H₁₇S [M – F] 349.1046 found 349.1049.

(Z)-2-Fluoro-1-(2-methoxy-9H-fluoren-9-ylidene)-2-methyl-2,3-dihydro-1H-benzo[b]cyclopenta[d]thiophene (**25b**).

A mixture of **22** (195 mg, 0.89 mmol), P₄S₁₀ (295 mg, 1.33 mmol), Lawesson's reagent (537 mg, 1.33 mmol) in toluene (20 ml) was heated to 100 °C for 1 h. After TLC showed no remaining starting material, the dark green mixture was concentrated under reduced pressure and purified directly on a short column of silica gel (pentane : ethyl acetate – 20 : 1) to give a dark green oil. The oil was redissolved in toluene (20 ml) and freshly prepared 2-methoxy-9-diazo-9H-fluorene^[38] (278 mg, 1.24 mmol) was added portionwise over 5 min. The resulting mixture was left stirring overnight and HMPT (390 μ l, 347 mg, 2.12 mmol) was added afterwards. The mixture was stirred for an additional 24 h at room temperature. The crude reaction mixture was purified by column chromatography on silica gel (pentane : dichloromethane – 7 : 1) and recrystallization from ethanol to give the desired motor **Z-25b** as a yellow solid (190 mg, 0.48 mmol, 54%). Mp. (dec.) >200 °C. ¹H NMR (400 MHz, CD₂Cl₂): δ (ppm) 7.91 (d, J = 8.1 Hz, 1H), 7.76 (s, 1H), 7.70 (dd, J = 8.5, 8.5 Hz, 2H), 7.36 (dd, J = 7.5, 7.5 Hz, 1H), 7.27 (m, 2H), 7.20 (d, J = 8.0 Hz, 1H), 7.06 (d, J = 7.8 Hz, 1H), 6.98–6.90 (m, 2H), 3.99–3.80 (m, 4H), 3.42 (d, J = 15.1 Hz, 1H), 1.95 (d, J = 19.0 Hz, 3H). ¹³C NMR (100 MHz, CD₂Cl₂): δ (ppm) 159.7, 152.2 (d, J = 11.9 Hz), 143.9, 140.6, 140.4, 140.1, 138.5, 138.2, 134.3, 133.9, 129.0, 128.2, 127.0, 126.7, 125.3, 125.0, 124.9, 123.8, 120.6, 118.8, 113.8, 112.9 (d, J = 15.3 Hz), 108.2 (d, J = 198.5 Hz), 56.1, 46.1 (d, J = 26.9 Hz), 23.9 (d, J = 25.0 Hz). ¹⁹F NMR (376 MHz, CD₂Cl₂): δ (ppm) –132.6 (p, J = 17.9 Hz). HRMS (ESI): calcd for C₂₆H₁₉SO [M – F] 379.1151 found 379.1182.

Acknowledgements

This work was supported financially by the Netherlands Organization for Scientific Research (NWO-CW), The Royal Netherlands Academy of Arts and Sciences (KNAW), NanoNextNL of the Government of the Netherlands and 130 partners, the European Research Council (ERC; advanced grant no. 694345 to B.L.F.) and the Ministry of Education, Culture and Science (Gravitation program no. 024.001.035). The authors thank P. van der Meulen for assistance with NMR experiments.

Keywords: fluorine • molecular motor • quaternary • photoisomerization • unidirectional

- [1] M. Schliwa, Ed., *Molecular Motors*, VCH-Wiley, Weinheim, FRG, 2002.
- [2] M. Schliwa, G. Woehlke, *Nature* **2003**, *422*, 759–765.
- [3] K. Kinoshita, R. Yasuda, H. Noji, S. Ishiwata, M. Yoshida, *Cell* **1998**, *93*, 21–24.
- [4] M. Yoshida, E. Muneyuki, T. Hisabori, *Nat. Rev. Mol. Cell Biol.* **2001**, *2*, 669–677.
- [5] H. Itoh, A. Takahashi, K. Adachi, H. Noji, R. Yasuda, M. Yoshida, K. Kinoshita, *Nature* **2004**, *427*, 465–468.
- [6] P. D. Boyer, *Nature* **1999**, *402*, 247–249.
- [7] M. J. Pallen, N. J. Matzke, *Nat. Rev. Microbiol.* **2006**, *4*, 784–790.
- [8] H. C. Berg, *Annu. Rev. Biochem.* **2003**, *72*, 19–54.
- [9] H. C. Berg, R. A. Anderson, *Nature* **1973**, *245*, 380–382.
- [10] D. J. DeRosier, *Cell* **1998**, *93*, 17–20.
- [11] K. Kinbara, T. Aida, *Chem. Rev.* **2005**, *105*, 1377–1400.

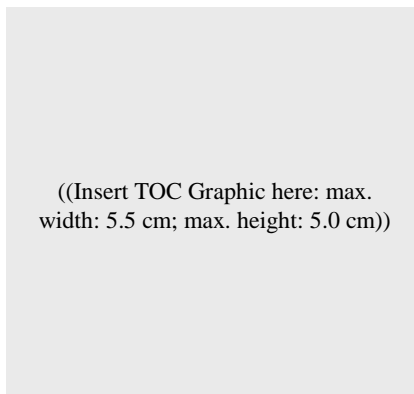
- [12] A. Coskun, M. Banaszak, R. D. Astumian, J. F. Stoddart, B. A. Grzybowski, *Chem. Soc. Rev.* **2012**, *41*, 19–30.
- [13] V. Balzani, A. Credi, M. Venturi, *Molecular Devices and Machines - Concepts and Perspectives for the Nanoworld*, VCH-Wiley, Weinheim, **2008**.
- [14] S. Erbas-Cakmak, D. A. Leigh, C. T. McTernan, A. L. Nussbaumer, *Chem. Rev.* **2015**, *115*, 10081–10206.
- [15] A. Livoreil, J.-P. Sauvage, N. Armaroli, V. Balzani, L. Flamigni, B. Ventura, *J. Am. Chem. Soc.* **1997**, *119*, 12114–12124.
- [16] J.-P. Sauvage, *Molecular Machines and Motors. Structure and Bonding*, Springer-Verlag, Heidelberg, **2001**.
- [17] J. F. Stoddart, *Chem. Soc. Rev.* **2009**, *38*, 1802.
- [18] M. Jiménez, C. Dietrich-Buchecker, J. Sauvage, *Angew. Chem. Int. Ed.* **2000**, *39*, 3284–3287.
- [19] A. H. Flood, J. F. Stoddart, D. W. Steuerman, J. R. Heath, *Science* **2004**, *306*, 2055–6.
- [20] C. J. Bruns, J. F. Stoddart, *Acc. Chem. Res.* **2014**, *47*, 2186–99.
- [21] J. F. Stoddart, *Acc. Chem. Res.* **2001**, *34*, 410–411.
- [22] H. L. Tierney, C. J. Murphy, A. D. Jewell, A. E. Baber, E. V. Iski, H. Y. Khodaverdian, A. F. McGuire, N. Klebanov, E. C. H. Sykes, *Nat. Nanotechnol.* **2011**, *6*, 625–9.
- [23] C. J. Murphy, E. C. H. Sykes, *Chem. Rec.* **2014**, *14*, 834–840.
- [24] E. C. H. Sykes, *Angew. Chem. Int. Ed.* **2012**, *51*, 4277–4278.
- [25] T. J. Huang, B. Brough, C.-M. Ho, Y. Liu, A. H. Flood, P. A. Bonvallet, H.-R. Tseng, J. F. Stoddart, M. Baller, S. Magonov, *Appl. Phys. Lett.* **2004**, *85*, 5391.
- [26] T. Kudernac, N. Ruangsapichat, M. Parschau, B. Maciá, N. Katsonis, S. R. Harutyunyan, K.-H. Ernst, B. L. Feringa, *Nature* **2011**, *479*, 208–211.
- [27] W. R. Browne, J. J. D. de Jong, T. Kudernac, M. Walko, L. N. Lucas, K. Uchida, J. H. van Esch, B. L. Feringa, *Chem. - A Eur. J.* **2005**, *11*, 6430–6441.
- [28] W. R. Browne, J. J. D. de Jong, T. Kudernac, M. Walko, L. N. Lucas, K. Uchida, J. H. van Esch, B. L. Feringa, *Chem. - A Eur. J.* **2005**, *11*, 6414–6429.
- [29] O. Ivashenko, J. T. Van Herpt, B. L. Feringa, P. Rudolf, W. R. Browne, *J. Phys. Chem. C* **2013**, *117*, 18567–18577.
- [30] O. Ivashenko, J. T. Van Herpt, B. L. Feringa, P. Rudolf, W. R. Browne, *Langmuir* **2013**, *29*, 4290–4297.
- [31] O. Ivashenko, J. T. van Herpt, P. Rudolf, B. L. Feringa, W. R. Browne, *Chem. Commun.* **2013**, *49*, 6737–6739.
- [32] J. Areephong, W. R. Browne, N. Katsonis, B. L. Feringa, *Chem. Commun.* **2006**, *100*, 3930–3932.
- [33] J. Areephong, T. Kudernac, J. J. D. de Jong, G. T. Carroll, D. Pantorott, J. Hjelm, W. R. Browne, B. L. Feringa, *J. Am. Chem. Soc.* **2008**, *130*, 12850–12851.
- [34] H. Logtenberg, J. Areephong, J. Bauer, A. Meetsma, B. L. Feringa, W. R. Browne, *ChemPhysChem* **2016**, *17*, 1895–1901.
- [35] J. Vicario, M. Walko, A. Meetsma, B. L. Feringa, *J. Am. Chem. Soc.* **2006**, *128*, 5127–5135.
- [36] J. Vicario, A. Meetsma, B. L. Feringa, *Chem. Commun.* **2005**, *116*, 5910.
- [37] M. M. Pollard, A. Meetsma, B. L. Feringa, *Org. Biomol. Chem.* **2008**, *6*, 507–512.
- [38] J. Bauer, L. Hou, J. C. M. Kistemaker, B. L. Feringa, *J. Org. Chem.* **2014**, *79*, 4446–4455.
- [39] M. Klok, N. Boyle, M. T. Pryce, A. Meetsma, W. R. Browne, B. L. Feringa, *J. Am. Chem. Soc.* **2008**, *130*, 10484–10485.
- [40] D. W. Smith, *Inorganic Substances: A Prelude to the Study of Descriptive Inorganic Chemistry*, Cambridge University Press, **1990**.
- [41] B. Zajc, R. Kumar, *Synthesis* **2010**, *2010*, 1822–1836.
- [42] E. Differring, M. Wehrli, *Tetrahedron Lett.* **1991**, *32*, 3819–3822.
- [43] A. K. Ghosh, B. Zajc, *Org. Lett.* **2006**, *8*, 1553–1556.
- [44] E. Differding, G. M. Rügge, *Tetrahedron Lett.* **1991**, *32*, 3815–3818.
- [45] N. Koumura, E. M. Geertsema, A. Meetsma, B. L. Feringa, *J. Am. Chem. Soc.* **2000**, *122*, 12005–12006.
- [46] N. Koumura, E. M. Geertsema, M. B. van Gelder, A. Meetsma, B. L. Feringa, *J. Am. Chem. Soc.* **2002**, *124*, 5037–5051.
- [47] Calculated from the experimental data available in our group.
- [48] M. M. Pollard, P. V. Wesenhagen, D. Pijper, B. L. Feringa, *Org. Biomol. Chem.* **2008**, *6*, 1605.
- [49] A. C. Coleman, J. Areephong, J. Vicario, A. Meetsma, W. R. Browne, B. L. Feringa, *Angew. Chem. Int. Ed.* **2010**, *49*, 6580–6584.
- [50] T. Fernandez Landaluce, G. London, M. M. Pollard, P. Rudolf, B. L. Feringa, *J. Org. Chem.* **2010**, *75*, 5323–5325.

Entry for the Table of Contents (Please choose one layout)

Layout 1:

FULL PAPER

Text for Table of Contents



Author(s), Corresponding Author(s)*

Page No. – Page No.

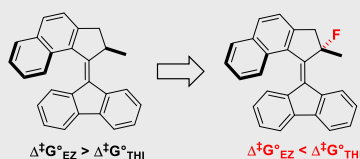
Title

Layout 2:

FULL PAPER

Peter Štacko, Jos C. M. Kistemaker,
Ben L. Feringa*

Page No. – Page No.

Fluorine-substituted molecular
motors with a quaternary stereogenic
center

A series of overcrowded alkenes with a quaternary stereogenic center substituted with fluorine was investigated for application as unidirectional molecular motors. Major increase of the thermal isomerization barrier was found as a consequence of substituting hydrogen for fluorine atom.